REPORT DOCUMENTATION PAGE

Form Approved
OMB No. 0704-0188

AD-A265 269

2. REPORT DATE	3. REPORT TYPE AND DATES COVERED
5/18/93	Interim, 6/1/92-5/31/93

4. TITLE AND SUBTITLE
Adsorption and Dissociation of Disilane on Si(001) Studied by STM

5. FUNDING NUMBERS
Grant
N00014-91-J-1629
R&T Code
41 S001

6. AUTHOR(S)
M. Bronikowski, Y. Wang, M. McEllistrem, D. Chen and R. J. Hamers

7. PERFORMING ORGANIZATION NAME(S) AND ADDRESS(ES)
Department of Chemistry
University of Wisconsin-Madison
1101 University Avenue
Madison, WI 53706-1396

8. PERFORMING ORGANIZATION REPORT NUMBER

9. SPONSORING / MONITORING AGENCY NAME(S) AND ADDRESS(ES)
Office of Naval Research, Chemistry
800 North Quincy Street
Arlington, VA

10. SPONSORING / MONITORING AGENCY REPORT NUMBER
12

DTIC ELECTE JUN 01 1993 S E D

11. SUPPLEMENTARY NOTES

12a. DISTRIBUTION / AVAILABILITY STATEMENT
Unlimited

93-12154

93 5 25 037

13. ABSTRACT (Maximum 200 words)

The surface-adsorbed fragments resulting from the room-temperature adsorption and dissociation of disilane (Si_2H_6) on Si(001) are observed and identified using Scanning Tunneling Microscopy (STM). The predominant fragments are H and SiH_2, which are identified by the symmetries of their binding sites on the surface. H atoms often bind near single or double dimer vacancy defects, while SiH_2 tends to bind near C-type defects. We find that adsorbed H atoms induce buckling of the dimer rows on the Si(001) surface, while SiH_2 groups do not. This difference is ascribed to differences in the electronic structure of the two surface-bound species. No systematic correlation between the positions of the H atoms and SiH_2 groups is evident, which indicates that the fragments of a single disilane molecule are not localized in a small region. This fact suggests that at least some of the molecular fragments from disilane dissociation are mobile on the Si(001) surface at room temperature. Further decomposition of the SiH_2 fragments can be induced by annealing, which produces surface structures similar to those seen in molecular-beam epitaxial growth of silicon: small asymmetric islands form with low disilane coverages, whereas higher coverages give multilayer island growth.

14. SUBJECT TERMS	15. NUMBER OF PAGES
Scanning tunneling microscopy, STM, surfaces, semiconductors, photovoltage, silicon.	44 total
	16. PRICE CODE ---

17. SECURITY CLASSIFICATION OF REPORT	18. SECURITY CLASSIFICATION OF THIS PAGE	19. SECURITY CLASSIFICATION OF ABSTRACT	20. LIMITATION OF ABSTRACT
Unclassified	Unclassified	Unclassified	UL

U.S. OFFICE OF NAVAL RESEARCH

GRANT N00014-91-J-1629

R&T Code 413S001

Technical Report #12

Adsorption and Dissociation of Disilane on Si(001) Studied by STM

by

M. Bronikowski, Y. Wang, M. McEllistrem, D. Chen, and R.J. Hamers

Prepared for Publication

in

Surface Science

May 18, 1993

Department of Chemistry
University of Wisconsin-Madison
Madison, WI 53706

Adsorption and Dissociation of Disilane on Si(001) Studied by STM

Michael J. Bronikowski, Yajun Wang, Marcus T. McEllistrem, Dong Chen and Robert J. Hamers*

Department of Chemistry
University of Wisconsin
1101 University Avenue
Madison, Wi 53706

Abstract

The surface-adsorbed fragments resulting from the room-temperature adsorbtion and dissociation of disilane (Si_2H_6) on Si(001) are observed and identified using Scanning Tunneling Microscopy (STM). The predominant fragments are H and SiH_2, which are identified by the symmetries of their binding sites on the surface. H atoms often bind near single or double dimer vacancy defects, while SiH_2 tends to bind near C-type defects. We find that adsorbed H atoms induce buckling of the dimer rows on the Si(001) surface, while SiH_2 groups do not. This difference is ascribed to differences in the electronic structure of the two surface-bound species. No systematic correlation between the positions of the H atoms and SiH_2 groups is evident, which indicates that the fragments of a single disilane molecule are not localized in a small region. This fact suggests that at least some of the moleular fragments from disilane dissociation are mobile on the Si(001) surface at room temperature. Further decomposition of the SiH_2 fragments can be induced by annealing, which produces surface structures similar to those seen in molecular-beam epitaxial growth of silicon: small asymmetric islands form with low disilane coverages, whereas higher coverages give multilayer island growth.

*To whom correspondence should be addressed

Introduction

Epitaxial growth of Si(001) by chemical vapor deposition (CVD) is important in a wide variety of semiconductor electronics and thin film technologies. CVD by disilane deposition and thermal decomposition is particularly relevant because of this molecule's relatively high sticking coefficient and low activation barrier for decomposition. An understanding of the fundamental chemistry and physics of the decomposition of disilane on silicon is thus important in controlling and utilizing the epitaxial growth process. The Si_2H_6/Si(001) system is also fundamentally interesting as a prototypical surface chemical reaction. While adsorption of disilane and similar molecules on Si(001) has been investigated with a number of surface science techniques [1-5], the presence of several similar (but chemically distinct) molecular fragments on the surface has made studying the reaction chemistry difficult. Additionally, the presence of steps and defects on this surface has made it difficult to identify the fragments and the reaction pathways. Previous STM studies have shown that the unique bonding configurations at these sites leads to heterogeneous electronic properties [6, 7], suggesting that steps and defects might also play an important role in the reaction chemistry.

The importance of disilane as a semiconductor precursor material has lead several researchers to study the interaction of disilane with Si(001) at higher coverages and high temperatures. Boland used STM to investigate the role of hydrogen bonding and desorption in the CVD process, using both disilane [8] and atomic

hydrogen [9-11] to dose Si(100) surfaces with hydrogen. One of these investigations, carried out with saturation coverages of Si_2H_6, showed that under conditions of continuous exposure, multilayer epitaxial growth occurs at least in part by direct reaction between disilane and the monohydride-terminated Si(001) surface [8]. Lin et al. [12] also investigated the growth of silicon from disilane on Si(001); they found that annealing disilane-covered surfaces to elevated temperatures produced anisotropic islands, which they attributed to a silicon monohydride specie.

While these previous studies identified important properties of the silicon growth, many important aspects of the *chemistry* of disilane on silicon have not yet been elucidated. Especially lacking has been an understanding of the initial steps in the process of adsorption, dissociation, and epitaxial growth, such as the fragmentation pattern of the disilane molecule on the surface, the identities and binding geometries of the fragments formed, and the mechanism by which the fragmentation occurs. In order to more fully elucidate the bonding and reaction chemistry of disilane, we have investigated the adsorption and dissociation of disilane on Si(001) with particular emphasis on identifying the surface molecular fragments and their bonding geometries. We find that after room temperature adsorption the surface species are mainly H and SiH_2, both of which can be identified based on the symmetry of the binding sites with respect to the Si(001) 2x1 surface. The distribution of these fragments on the surface and their proximity to each other and to surface defects provides further information on the dissociation process. By heating disilane-dosed silicon surfaces, we

can also observe directly the epitaxial growth of silicon from these adsorbed disilane fragments. We find that this process is similar in many ways to growth from pure silicon.

Experimental

Our STM apparatus, along with controlling electronics, have been described previously [13, 14]. All experiments are carried out at room temperature in an ion-pumped UHV stainless steel chamber (base pressure $<10^{-10}$ Torr). Our STM apparatus consists of an electrochemically etched tungsten tip mounted on a PZT piezoelectric tube scanner (Staveley Sensors, Inc.), which is attached to the end of an Inchworm motor (Burleigh Instruments) for coarse approach. In tunneling experiments, voltages are applied to the sample in an electrically isolated tunneling stage. Samples can be heated resistively on a separate heating stage by passing current directly through the sample. Disilane is introduced into the chamber through a precision leak valve.

Samples of *n*-type Si(001) wafers (polished to within 0.25 degree; Virginia Semiconductor) are degassed for 10 - 12 hours at 700 °C, then heated for 1 - 2 seconds to 1150 °C to remove any silicon oxides and contaminants. After the silicon cools to room temperature (about 1 hour), it is transferred to the tunneling stage. The tungsten tip is brought into tunneling range and the surface is imaged to check that it is well ordered and free from contamination and to verify the 2x1 reconstruction of the Si(001) surface prior to dosing with disilane. The tip is then withdrawn and the sample is

exposed to a selected pressure (typically 10^{-8} Torr to 10^{-6} Torr as measured by an uncalibrated ion gauge, depending on the desired coverage) of 10% disilane in helium (Voltaix, Inc.; 99.5% disilane purity, with silane, SiH_4, being the primary impurity) for 100 - 200 seconds. With a reported room temperature sticking coefficient of approximately 0.1 [12, 15], exposure conditions can be chosen to obtain coverages from a few percent of a monolayer to several monolayers of disilane. The tip is brought back into tunneling and the disilane-dosed surface is imaged.

Images are typically recorded with a tunneling current of 0.3 - 1.0 nA and voltage magnitude of 1.4 - 3.0 volts. Images can be taken with either negative or positive sample voltage polarity, which yield images of the filled or unfilled surface electronic states, respectively. Large scale STM images showed that the average terrace width on the surface is greater than 500 Å, corresponding to a misalignment from the (001) plane of less than 0.14 degrees.

Results

I. Identification and Local Bonding Geometry of Dissociation Fragments

Figure 1 shows a typical image of clean Si(001) taken with negative sample bias. This image shows the well known dimer row structure of the 2x1 reconstruction of this surface, with individual Si dimers resolved. In this filled-state image, tunneling current originates primarily from the occupied π-type bonding orbital

between adjacent pairs of silicon atoms, so that the dimers are oval in shape with a maximum height between the two atoms of each dimer [16]. Also visible are typical surface defects such as single and double dimer vacancies [6, 7]. Figure 2 shows a filled state, negative bias image of the Si(001) surface after dosing with disilane. While the underlying dimer row structure of the Si(001) surface is still prominent, one immediately notices a large number of new features on the surface. While the structure of these fragements will be discussed in more detail below, we note two important facts here: first, the characteristic features produced by dosing appear to be rather randomly distributed across the surface, showing no strong preference for steps. Secondly, these features virtually all appear as protrusions from the surface, where as the original defects present on the surface were virtually all depressions. Thus, distinguishing the features produced by dosing is rather straightforward despite the relative complexity of the starting surface.

As the surface coverage is increased, the number of these defects increases approximately linearly. At high exposures, the surface coverage saturates, leading to a surface such as that shown in figure 3. Even at this saturation coverage, however, short-range order is still clearly visible in the STM images and can be identified as fuzzy second-order spots (7.7 Å periodicity) in 2-dimensional Fourier Transforms of the STM images, indicating that the Si-Si dimer bond is not broken by the adsorption of disilane.

In order to identify the adsorbed entities on this surface, we now turn attention to high-resolution images at much lower exposure. At these lower exposures, the molecular fragments are

isolated from each other, greatly simplifying the analysis. It becomes clear that the seemingly-complicated surface observed at higher coverages results from only a few isolated molecular fragments. Since STM primarily probes the electronic structure of the surface, bias-dependent STM imaging is an important element in separating and identifying the various species present on the surface. Figure 4 shows an image of disilane-dosed Si(001) acquired at positive sample bias. In this case, electrons tunnel from the tip and into the unoccupied π^* antibonding orbital of the Si dimers. As has been noted [16], this π^* antibonding orbital is characterized by a nodal plane midway between the two atoms of the dimer; as a consequence, each dimer of the clean surface now appears as two well-resolved protrusions. Again, exposure to SiH_2 produces new characteristic features which we associate with adsorbed molecules or fragments of dissociation.

In attempting to identify the adsorbate-induced features seen in such images, it is useful to consider the possible dissociation fragments from disilane molecules and their binding geometries on the surface. Previous studies [1, 17] have shown that disilane dissociatively chemisorbs on Si(001) yielding SiH_3, which decomposes further at room temperature (under low coverage conditions) to form SiH_2 and H. The extent of dissociation appears to be controlled by the H coverage, so that at low coverage the dissociation is expected to be more complete. Thus, we expect the predominant surface species to be adsorbed H atoms and adsorbed SiH_2 fragments, present in roughly equal amounts.

Because the STM is primarily sensitive to the local electronic structure of the surface and because the electronic structure of isolated molecular entities such as adsorbed SiH_2 and SiH_3 groups are not known, one cannot make an absolute identification of the fragments from their appearance alone. However, we note that an important driving force behind semiconductor surface reconstructions is the minimization of the surface free energy through the optimization of four-fold coordination for all silicon atoms: i.e., the elimination of surface "dangling bonds". Since the adsorbed species are also covalently-bonded Si-containing species, it is reasonable to assume that these same principles should also be important for adsorbed species as well. If the lowest-energy binding locations for the fragments corresponds to the locations which maximize four-fold coordination, then one should be able to infer the identity of the fragments from their bonding location. Thus, we have established a systematic way of identifying molecular fragments in which we infer the coordination from the bonding location, and we infer the fragment identify from the surface coordination.

To illustrate what we expect to see for the various surface fragments, Figure 5 shows the most likely high-symmetry binding geometries for adsorbed H atoms and SiH_2 fragments. Figure 5a shows how isolated H atoms may bind to the surface: an H atom can break the Si-Si π bond and bond to either of the two atoms of the dimer, leaving the other atom with a singly-occupied dangling bond, as shown. One could also find both atoms of the same dimer bonded to H atoms, as shown, forming a region of local "(2x1) monohydride". Both these geometries have been observed by Boland for silicon

dosed with atomic hydrogen [9, 10]. For an adsorbed SiH_2, achieving four-fold coordination requires forming two bonds to the surface, which figure 5b shows can be done is three high-symmetry ways, corresponding to the SiH_2 bonding between two dimers of the same dimer row, bonding between dimers of neighboring rows, or bridging the atoms of a single dimer. It should also be noted that because the Si-Si dimers are held together by a strong σ bond and a weak π bond, a bond formed between a dimer atom and an adsorbate leaves the strong σ bond intact, so that the spacing between the Si atoms within the dimer is not strongly affected by adsorption; this will be discussed in more detail below.

We now focus on a more detailed analysis of the STM images after exposure to Si_2H_6. While disilane-dosed surfaces such as those shown in Figures 2 - 4 may appear quite complex and unstructured on first viewing, examination of a large number of such images reveals this impression is incorrect; in fact, virtually all of the structures on the surface arise from only *two* characteristic features, while larger structures are formed from collections of these features. One such feature consists of a bright spot surrounded by a dark ring, sitting among the dimer rows on the surface. Figure 6 shows a section of disilane-dosed surface upon which several of these features can be seen, as indicated. This feature is also seen many times in figure 2. An single example of this feature is shown in an enlarged view in figure 7. The topography of this feature can be seen more quantitatively in figure 8, which shows a linescan through one of these features. The central bright area extends about 0.7 Å above the surrounding silicon surface, and it sits in a depression

approximately 2 dimer units wide and 0.55 Å deep. Careful examination of figure 7 reveals the bonding symmetry of this feature on the surface, from which we can deduce its identity. The bright spot sits upon one dimer row, offset from the center of that row, as indicated by the overlaid horizontal grid lines. It is also apparent that the feature's horizontal position does not correspond to the position of a dimer in this dimer row. Rather, the spot sits symmetrically between the expected positions of two dimers in this row, as indicated by the vertical grid lines.

Consideration of Figure 5b shows that the above binding symmetry is just that expected for one possible configuration of SiH_2, that in which SiH_2 bridge-bonds between two dimers within a single row. Because the formation of a bond between an SiH_2 and a dimer breaks the weak Si-Si dimer π-bond but does not break the stronger σ-bond, to a first approximation the geometry of the underlying Si substrate will not be significantly changed by adsorption of an SiH_2 group. In particular the Si-Si bond length should not change significantly in dimers bonded to SiH_2 groups, and thus the adsorbate should be positioned over the dimer row as shown; this is consistent with our observations.

In fact, this is the only sterically reasonable configuration of the three possible sites shown in Figure 5b. In bulk silicon the Si-Si bond length is 2.35 Å [18] (the disilane Si-Si bond length is approximately 2.3 Å [18]). On the *unreconstructed*, ideally terminated bulk Si(001) surface, the tetrahedral bonding angle of 109.5 degrees implies a surface Si atom separation of 3.84 Å. On the *reconstructed* surface, alternate rows of atoms shift towards each

other, forming dimer pairs, but the atoms do not shift in a direction parallel to the dimer rows (see figure 4). Thus the distance between dimers of the same row will still be 3.84 Å while the distance between the centers of adjacent rows will be just twice this length, or 7.68 Å. Pollmann et al. [19] have calculated the Si dimer bond length at ≤ 2.35 Å, which implies a separation between nearest neighbor atoms of adjacent rows of at least 7.68 - 2.35 = 5.33 Å. Assuming as above that the dimer bond length does not change significantly upon bonding to an SiH_2 group, tetrahedral geometry implies that a dimer bridging two adjacent rows would result in Si-Si σ-bond lengths of 3.26 Å, much longer than either the bulk silicon or molecular disilane bond lengths. Even the maximum bond angle of 180 degrees gives Si-Si bond lengths of 2.66 Å! On the other hand, an SiH_2 group bridging two dimers of the same row with tetrahedral geometry would have Si-Si bond lengths equal to that of bulk silicon because in this configuration the relative positions of the substrate atoms involved in bonding are not different than in the bulk. One therefore expects that SiH_2 will be much more stable on the latter site than on the former. The third possibility, the bridging of a single dimer by an SiH_2 group, would result in bonding angles of about 60 degrees, clearly very sterically unfavorable. Thus dimer bridging within a row appears to be the most favorable arrangement for the adsorbed SiH_2 from a purely steric standpoint. We conclude that the feature shown in figure 7 is an SiH_2 group, bound to the surface in this geometry.

STM images at positive sample bias show an adsorption-induced fragment with the same symmetry as that described above:

again, the fragment appears as a small protrusion surrounded by a depression. An example of this is shown in figure 9, which is an enlarged view of a section of figure 4. From STM images of identical areas at positive and negative sample bias, we have established that they are indeed the same fragment, and both represent an adsorbed SiH_2 group in the bridge-bonded position as described above. While at negative bias the SiH_2 fragment produces central protrusion extending above the Si dimers approximately 0.7 Å, at positive bias the protrusion is less pronounced.

Another feature that occurs commonly in positive-bias images can also be seen in figure 9. These features consist of a bright spot at one end of a dimer, with a depression on the other side of that dimer. Both the bright spot and the dark area have the same symmetry with respect to the surface: they sit directly on top of a Si atom, i.e., they lie on a dimer row displaced to one side and sit on top of one dimer rather than between two. Figure 5a shows that this is just the symmetry that hydrogen atoms should show when bound to the surface. Boland observed similar features in STM experiments on Si(001) surfaces dosed with atomic hydrogen and identified these features with adsorbed H atoms [8-10]. He suggested that the appearance of the hydrogen atoms could be explained as follows. When a hydrogen atom breaks a Si-Si π-bond and binds to one of the silicon atoms, it leaves a singly occupied dangling bond orbital on the other Si atom. Boland's scanning tunneling spectroscopy (STS) measurements [8, 10] showed that this orbital has more electron density in the vicinity of the Fermi level than a Si-Si π-bond, while the Si-H σ-bond has less density than the π-bond. Thus, the dangling

bond should appear brighter on the STM image than the background dimer rows, while the adsorbed H atom should appear less bright than the background. We observe features similar to those seen by Boland, and so we conclude that the bright spots on our images correspond to dangling bonds, with the adjacent dark areas corresponding to adsorbed hydrogen atoms.

We can also identify hydrogen atoms in negative-bias images. Several examples are shown in figure 10. Here again we see a bright area next to a dark area on the same dimer, with the same symmetry as discussed above for H atoms. We conclude as above that such features show the presence of single adsorbed H atoms. It is also apparent at negative bias that these features are associated with a longer range change in the structure of the surface, as discussed in the next section.

For further evidence as to the identity of the features observed, we have performed experiments where silicon samples were dosed with a few percent of a monolayer of disilane (10^{-8} Torr, 200 sec.), heated to about 500 K for 5 minutes and allowed to cool before imaging. On these surfaces we found that the SiH_2 groups disappeared whereas some surface hydrogen remained, and small asymmetric features with dimensions of a few dimer widths formed. These features appear to be islands of silicon one dimer row wide and three to five dimers long. The observation of these islands, present at about the expected density, gives additional support to our interpretation of the features in figures 2 - 10 as disilane fragments, rather than defects or contamination. The decomposition

of disilane fragments and growth of silicon upon heating of the surface is discussed more fully in section IV.

II. Dimer Buckling and Charge Exchange

Figure 10 shows that the dimers in rows containing an H atom are "buckled": alternate dimers have most of their intensity on alternate sides of the dimer row (alternate atoms). This dimer buckling is ultimately due to the breaking of the mirror symmetry down the center of the dimer row caused by the binding of an H atom on one side of the row. It arises from a combination of electronic and geometric effects in the following way.

When the structure of a dimer is changed in a manner resulting in a non-symmetric distribution of charge between the two atoms of the dimer (as happens, for example, when an H atom is bonded to only one of the two atoms, or at a C-type defect), interaction with the resulting dipole causes the electron clouds on adjacent (nearest neighbor) dimer pairs to rearrange in a way that maximizes charge separation: charge on these nearest neighbors will shift to the atom farthest from the highest charge density on the original dimer, and so the dipoles on the neighbors will be antiparallel to the dipole on the original dimer. The next dimers in the row interact with these nearest neighbors, aligning their dipoles in the opposite direction, and so on, so that the entire row takes on a zig-zagged electronic structure.

The charge rearrangement is accompanied by a geometric, structural change: a dimer tilts in the vertical plane so that the atom with higher electron density moves higher in the plane of the surface and the other atom moves lower. This means that the higher atom will have a higher density of filled electronic states (thus showing bright on filled-state STM images), while the lower atom will have a higher density of unfilled states and will be brighter on unfilled-state images. Thus, in filled state images, the geometric and electronic effects enhance each other: the higher atoms have a higher state density, and so appear much brighter than the lower atoms. This results in the pronounced zig-zag structure observed in these dimer rows in negative-bias images such as Figure 10. In empty-state images, on the other hand, the geometric and electronic effects work in opposite directions and tend to cancel: the atoms that are farther away from the STM tip have a higher density of electronic states involved in tunneling. Thus the dimer buckling in rows containing an H atom is not very pronounced in positive-bias images, as is apparent in Figure 9.

Inspection of figures 6, 7, and 10 reveals that H atoms induce considerable buckling on the surface, whereas SiH_2 groups do not give any appreciable buckling even though they clearly break the mirror-plane symmetry along the center of the dimer row. This can be understood from the above discussion. Hydrogen is more elctronegative than silicon (Pauling electronegativities 2.20 and 1.90, respectively [20]) and thus an H atom on the surface should withdraw charge from the bonded Si atom [21]. This charge withdrawal would induce a dipole between the Si atoms of that

dimer, which would lead to buckling of that dimer row as discussed above. SiH_2, on the other hand, would not behave in this way when bonded to the surface. The resulting Si-Si bond between surface and adsorbate is symmetric and so no charge transfer should occur. Thus an SiH_2 group should not induce buckling on the surface, in agreement with our observations.

Similar effects have been observed in STM studies of a number of species adsorbed on Si(001) and suggest that the direction and magnitude of buckling are directly correlated with the direction and magnitude of charge transfer between surface Si atoms and adsorbed species. Boland [22] found that chlorine atoms induce dimer row buckling and tend to bond on the lower of the two atoms of a dimer. This is what we observe for H atoms, and is the behavior expected for a charge-withdrawing specie. Several groups have studied alkali metals on Si(001), in particular lithium, potassium and cesium [23-25] and find that these metals induce buckling and bond to the *higher* of the two dimer atoms. Lin et al. observed this same effect in the bonding of silver to Si(001) [26]. These metals are strongly electron donating, and so increase the charge density on the Si atoms to which they bond. The dimers thus tend to tilt so that the Si atoms bonded to the metal adsorbates are above the surface.

Figures 2 - 10 show that H and SiH_2 tend to bind to the surface on flat terraces, rather than at or near step edges, and that they tend to be located near defects. SiH_2 tends to bind near C-type defects, as can be seen in figures 2 and 6. Most of the features identified as SiH_2 groups in these figures are bound next to what appear to be C-type defects, and this is the general trend observed. We also observe

that the dangling-bond sites created on two dimers as a result of SiH_2-bonding do not appear bright on filled-state images, as do the dangling bonds next to H atoms. Evidently, the electron density on these dangling-bond orbitals is either not as great or is at energies farther from the Fermi level when SiH_2 bonds than when hydrogen bonds to the surface, which is presumably an electronic effect. H atoms often, though not always, bind on dimers next to single or double dimer vacancy defects (A and B type defects, respectively). Examples of this can be found in figures 9 and 10. This behavior is consistent with a great deal of previous work: it is often found that surface defects play a dominant role in surface chemistry. It is known that the local electronic structure near defects differs from that of the rest of the surface [7], and it may be that the reactivity of defect sites results from this electronic structure. Future STS measurements will probe the correlation between electronic structure and reactivity on the Si(001) surface.

III. Mechanism of the Initial Dissociation of Disilane

By examining a large number of STM images like those shown here, we can draw some conclusions about the mechanism of the dissociation of Si_2H_6 on the Si(001) surface. We find no correlation among the positions of the various fragments, of a type that might indicate a concerted dissociation mechanism. The SiH_2 groups, for example, do not appear to be located closer to each other or to H atoms than one would expect for a random distribution of these fragments on the surface. Gates and Chiang [2] have recently

suggested that decomposition of disilane on Si(001) occurs by two competing reaction schemes:

$$Si_2H_6 \text{ --> } SiH_4 + \underline{\underline{Si}}H_2 \qquad (1)$$

and

$$Si_2H_6 \text{ --> } 2\underline{Si}H_3 \qquad (2)$$

(with $\underline{Si}H_3$ --> $\underline{\underline{Si}}H_2 + \underline{H}$ at room temperature),

where species are underlined to indicate bonding to the surface. Reaction (1) does not result in the deposition of hydrogen on the surface, while reaction (2) gives equal amounts of adsorbed H and SiH_2. We observe roughly equal numbers of adsorbed H atoms and SiH_2 groups, suggesting that reaction (2) is the dominant mechansim for dissociation. The lack of correlation between positions of SiH_2 groups suggests that either these groups or their SiH_3 precursors are mobile on the surface, at least when initially formed. This is energetically reasonable, as can be seen by considering the energetics of this reaction. Assuming, for example, that the SiH_3 groups are formed on adjacent dimers (not on the same dimer), we have:

$$\Delta E_{Total} = -\Delta E(H_3Si\text{-}SiH_3) - 2\Delta E(Si_{Surf}\text{-}SiH_3) + 2\Delta E(\text{dimer } \pi\text{-bond}). \qquad (3)$$

All of the Si-Si σ-bond strengths above have been estimated at 74 kcal/mol = 3.2 eV by Gates, Greenlief and Beach [1]. The dimer π-bond strength has been estimated by Boland [9] at 18 kcal/mole, or 0.8 eV per bond. Equation (3) then reduces to:

$$\Delta E_{Total} = -\Delta E(Si\text{-}Si) + 2\Delta E(\text{dimer } \pi\text{-bond}) \qquad (4)$$
$$= -3.2 \text{ eV} + 2(0.8 \text{ eV}) = -1.6 \text{ eV}$$

Reaction (2) thus yields about 1.6 eV of excess energy. Likewise, decomposition of SiH_3 on the surface gives:

$$\Delta E_{Total} = \Delta E(H\text{-}SiH_2) - \Delta E(Si_{Surf}\text{-}SiH_2) \qquad (5)$$
$$- \Delta E(Si_{Surf}\text{-}H) + 2\Delta E(\text{dimer } \pi\text{-bond})$$

Assuming that the bonding energies of hydrogen to the surface and to an SiH_2 group on the surface are approximately equal, we again have:

$$\Delta E_{Total} = -\Delta E(Si\text{-}Si) + 2\Delta E(\text{dimer } \pi\text{-bond}) = -1.6 \text{ eV} \qquad (6)$$

again yielding 1.6 eV of energy.

Wu and Carter [27] have calculated a barrier to H atom diffusion on the Si(001) surface, $E_D(H)$, of 2.0 eV, implying that hydrogen may not be able to diffuse from its site of formation in this reaction. On the other hand, Mo et al. [28] have measured an activation energy for Si atom diffusion on this surface of $E_D(Si) = 0.67 \pm 0.08$ eV, considerably less than the energy liberated by the

decomposition of an SiH_3 group. $E_D(SiH_2)$ is not known, but it is likely not much higher than $E_D(Si)$. It is thus reasonable to suggest that the barrier for SiH_2 diffusion is considerably less than the energy released upon the decomposition of an SiH_3 group. The excess energy might drive diffusion of SiH_2 groups away from their points of origin, which would explain the random distribution of these groups on the surface, relative both to each other and to H atoms on the surface.

These observations suggest that at room temperature, Si_2H_6 initially breaks into two SiH_3 groups, which decompose further to yield H and SiH_2, with the latter having enough energy to diffuse on the surface. This surface diffusion may also explain why SiH_2 adsorbates are usually found near C-type defects: if these defects are energetically favorable binding sites, such diffusion would allow fragments to move about the surface to find these sites. H atoms, of course, cannot diffuse to find favorable binding sites, according to the above energetics. Their preferential location near vacancy defects suggests that these defects are the preferred sites for dissociation of disilane molecules.

IV. Growth of silicon from disilane dissociation.

Further decomposition of the SiH_2 fragments can be produced by annealing. Figure 11 shows a typical surface produced by annealing a disilane-exposed surface to 500 Kelvin for 5 minutes. After annealing at this temperature, we no longer see any features which we can identify as SiH_2 groups. Instead, we observe

asymmetric islands, and on the terraces we also observe the same features which we previously attributed to adsorbed hydrogen atoms. While previous studies of disilane decomposition have suggested that islanding might occur by migration of SiH species to produce hydrogen-covered Si(001)-(2x1)H "monohydride" islands, our data do not support this interpretation. Instead, the island features appear to be identical to those previously observed from epitaxial growth of silicon (from pure Si). We base this conclusion on two pieces of evidence. First, the atomic-resolution images at negative sample bias show that the islands are comprised of bean-shaped structures, as can be observed in figure 12. Based on previous work for the monohydride surface, the distinction between islands of monohydride and islands of pure silicon should manifest itself most clearly in filled-state STM images: whereas the pure Si-Si dimers show a maximum state density at the center of the dimer bond, Hamers, Avouris and Bozso [16] showed that the Si(001)-(2X1) monohydride surface has a deep minimum at this location and therefore the local surface structure appears as two well-resolved protrusions. In contrast, empty-state images show a minimum at the center of the dimer bond *both* for clean- and for hydrogen-terminated silicon. Our work as well as the previous studies all show a maximum at the center of the Si-Si bond in filled-state images, and therefore we believe that all the experimental data to date supports islanding occurring *after* dissociation of the Si-H species, rather than before.

Secondly, we note that the corrugation profile across these islands shows a height change identical to that for a (001) step,

1.36Å. Figure 13 shows a corrugation profile across a 7-dimer-long island; the vertical scale was calibrated using a series of step edges and is believed to be accurate to within +-5%. Because of the lack of occupied Si-H states, if the islands were monohydride then one would expect the tip to move closer to the islands in order to achieve a constant tunneling current, and one would observe a height change between the islands and the surrounding terrace significantly smaller than the one observed. We thus conclude that the disilane fragments form islands of pure silicon upon annealing to 500 K, although it is possible that monohydride islands would be formed upon heating to lower temperatures.

The structures produced by growth from disilane are very similar to those produced from pure solid-phase epitaxial growth (i.e., molecular-beam epitaxy). Figure 14 shows a 2,500 x 1,000 Å image of a Si(001) surface grown by exposure to disilane at 1,000 Kelvin. In cases where the step density is very low, we note that growth occurs at least partially by island formation. In figure 14, we also observed that multilayer growth can occur. Closer inspection shows that each of the multilayer islands is pinned by an anti-phase boundary, in which the (2x1) reconstructions of the underlying layers are shifted by one lattice constant (3.84 Å) along either the (110) or (110) directions. Arrows point to the anti-phase boundaries, which can be clearly observed threading toward the multilayer islands. This kind of reconstruction-induced surface roughening in the case of island growth was previously observed by us for silicon surfaces grown by MBE techniques. Here, we see that

the same structural defects play an important role in the growth of smooth silicon surfaces by chemical vapor deposition.

Conclusions

We have studied the room temperature adsorption and dissociation of Si_2H_6 on Si(001) using STM. We identify H and SiH_2 fragments on the surface by the symmetry of their binding sites. Hydrogen atoms induce dimer row buckling on the surface, while SiH_2 groups do not, even though both species break the mirror-plane symmetry of a dimer row. This is believed to result from differences between the two species in adsorbate-substrate charge transfer. Hydrogen atoms often bind near single or double dimer vacancy defects, whereas SiH_2 groups usually bind near C-type defects. Neither specie binds preferentially at or near step edges. We observe no correlation among the locations of the various fragments on the surface, suggesting that surface dissociation is sufficiently exothermic to leave the SiH_2 fragments with enough energy to diffuse on the surface. This conclusion is in accord with estimates of the various relevant bond energies. Annealing disilane-covered surfaces produces pure silicon in the form of one-dimensional "dimer strings", while annealing at elevated temperatures during dosing leads to step growth and some island formation. Islands produced at higher growth temperatures are nearly always pinned by anti-phase domain boundaries in the underlying epitaxial layers.

Acknowledgments

MJB thanks the National Science Foundation for a postdoctoral research fellowship in chemistry. This work is supported in part by the U.S. Office of Naval Research.

References

[1] S. M. Gates, C. M. Greenlief and D. B. Beach, J. Chem. Phys. 93 (1990) 7493.

[2] S. M. Gates and C. M. Chiang, Chem. Phys. Lett. 184 (1991) 448.

[3] S. M. Gates and S. K. Kulkarni, Appl. Phys. Lett. 60 (1992) 53.

[4] Y. J. Chabal, Physica B 170 (1991) 447.

[5] P. Jakob, Y. J. Chabal and K. Raghavachari, Chem. Phys. Lett. 187 (1991) 325.

[6] R. J. Hamers, R. M. Tromp and J. E. Demuth, Phys. Rev. B 34 (1986) 5343.

[7] R. J. Hamers and U. K. Köhler, J. Vac. Sci Technol. A 7 (1989) 2854.

[8] J. J. Boland, Phys. Rev. B 44 (1991) 1383.

[9] J. J. Boland, J. Vac. Sci. Technol. A 10 (1992) 2458.

[10] J. J. Boland, Phys. Rev. Lett. 67 (1991) 1539.

[11] J. J. Boland, Surf. Sci. 261 (1992) 17.

[12] D.-S. Lin, *et al.*, Phys. Rev. B 45 (1992) 3494.

[13] X. Chen, *et al.*, Rev. Sci. Instrum. 63 (1992) 4308.

[14] M. McEllistrem, *et al.*, Phys. Rev. Lett. 70 (1993) 2471.

[15] S. M. Gates, Surf. Sci. 195 (1988) 307.

[16] R. J. Hamers, P. Avouris and F. Bozso, Phys. Rev. Lett. 59 (1987) 2071.

[17] Y. Suda, *et al.*, J. Vac. Sci. Technol. A 8 (1990) 61.

[18] R. C. Weast and M. J. Astle, ed. *CRC Handbook of Chemistry and Physics*. 62nd ed. 1982, CRC Press, Inc.: Boca Raton, Florida.

[19] J. Pollmann, *et al.*, Appl. Phys. A 41 (1986) 21.

[20] R. E. Dickerson, H. B. Gray and J. G. P. Haight, Chemical Principles. (W. A. Benjamin, Inc., Menlo Park, CA, 1974)

[21] P. Koke and W. Monch, Solid State Communications 36 (1980) 1007.

[22] J. J. Boland, Unpublished Results (1993)

[23] T. Hashizume, *et al.*, J. Vac. Sci. Technol. B 9 (1991) 742.

[24] T. Hashizume, *et al.*, J. Vac. Sci. Technol A 8 (1990) 233.

[25] Y. Hasegawa, *et al.*, J. Vac. Sci. Technol. A 8 (1990) 238.

[26] X. F. Lin, K. J. Wan and J. Nogami, Phys. Rev. B In Press (1993)

[27] C. J. Wu and E. A. Carter, Phys. Rev. B 46 (1992) 4651.

[28] Y.-W. Mo, *et al.*, Surf. Sci. 268 (1992) 275.

Figure Captions:

1) STM image of clean Si(001) obtained with -2V sample bias and 0.5 nA tunneling current. The area imaged is approximately 80 Å x 80 Å.

2) STM image (240 Å square) of Si(001) surface after exposure to 10 Langmuirs of a 10%/90% Si_2H_6/He mixture. A single-height atomic step runs through the image.

3) Image of Si(001) with saturation coverage Si_2H_6.

4) Positive-bias (empty-state) image of Si(001) showing characteristic surface features induced by Si_2H_6 adsorption. Imaging conditions: +2.0 V sample bias, 0.3 nA tunneling current, 150 Å x 150 Å.

5) Schematic illustration of likely high-symmetry bonding sites for a) adsorbed H atoms, and b) adsorbed SiH_2 groups on Si(001).

6) Negative-bias (filled-state) image of Si(001) showing characteristic surface features induced by Si_2H_6 adsorption. The features described in the text are indicated by arrows. Imaging conditions: -1.6 V sample bias, 1.0 nA tunneling current, 100 Å x 70 Å.

7) High-resolution filled-state STM image of adsorbed SiH_2 fragment showing its bridge-bonded position; grid lines denote boundaries of (2x1) unit cells of reconstructed Si(001) surface. Imaging conditions as in figure 6.

8) Constant-current topographic height contour across an SiH_2 group. The imaging conditions were as in figure 6.

9) High-resolution positive-bias (empty-state) STM image showing characteristic appearance of adsorbed H atoms and adsorbed SiH_2 groups. Imaging conditions: +2.0 V sample bias, 0.3 nA tunneling current, 75 Å x 75 Å.

10) High-resolution filled-state STM image showing both adsorbed H atoms and SiH_2 fragments. Imaging conditions: -1.4 V sample bias, 0.3 nA tunneling current, 75 Å x 65 Å.

11) Large-scale filled-state STM image showing islands produced by exposure of Si(001) to 2 Langmuirs of the 10% Si_2H_6/He mixture, followed by annealing to 500 Kelvin for 5 minutes. The image is skewed due to thermal drift during imaging.

12) High resolution filled-state image of island produced by annealing disilane-exposed Si(001) surface, showing bean-shaped structure characteristic of "clean" Si islands.

13) Height change measured across a 7-dimer-long "dimer string". The vertical height was calibrated against a series of step edges, which are 1.36 Å high.

14) 2,500 Å x 1,000 Å image of islands produced by growth of silicon from disilane at 1000 Kelvin. Multilayer islands are clearly visible. Their locations are pinned by anti-phase boundaries in the underlying epitaxial layers.

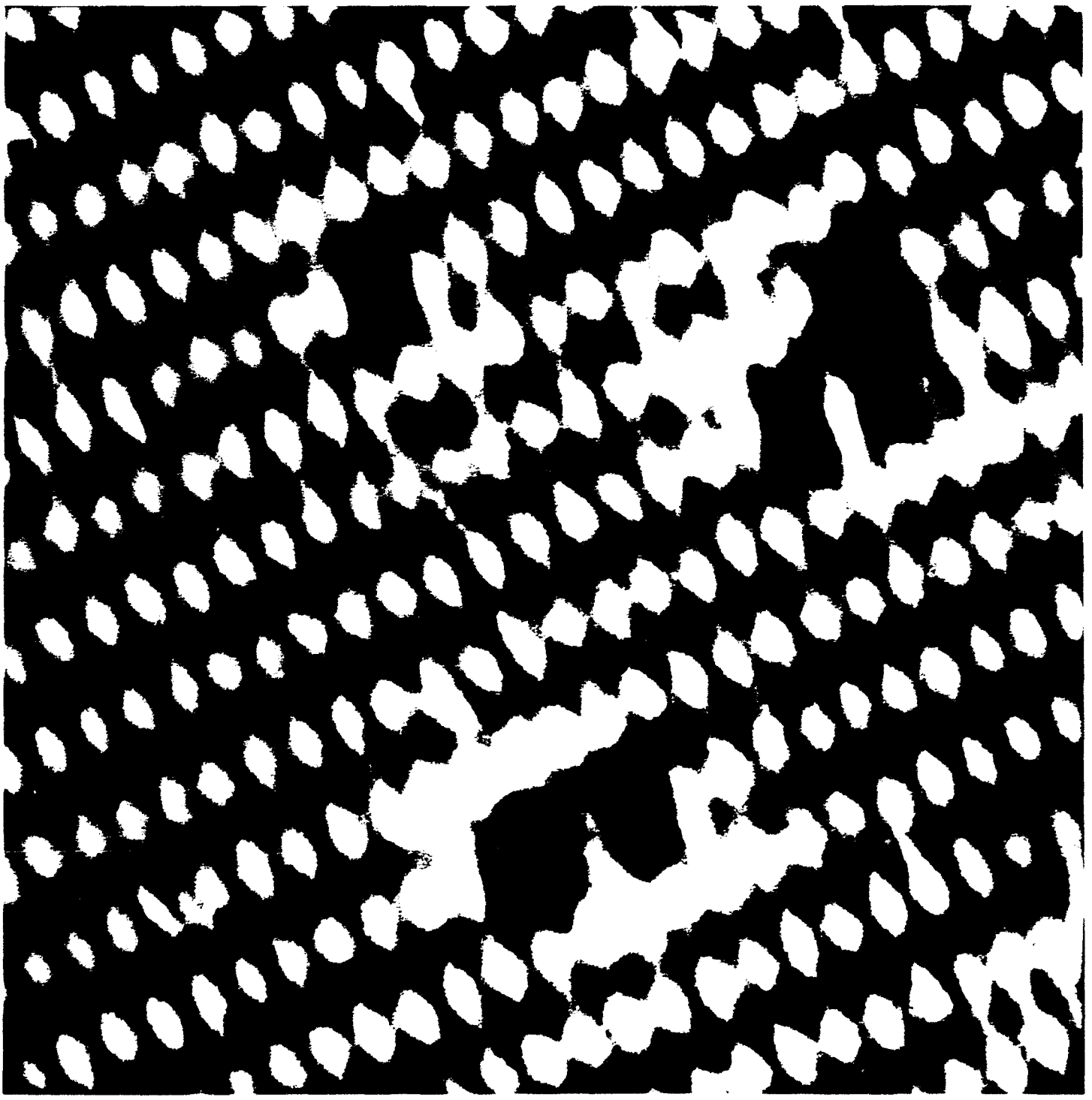

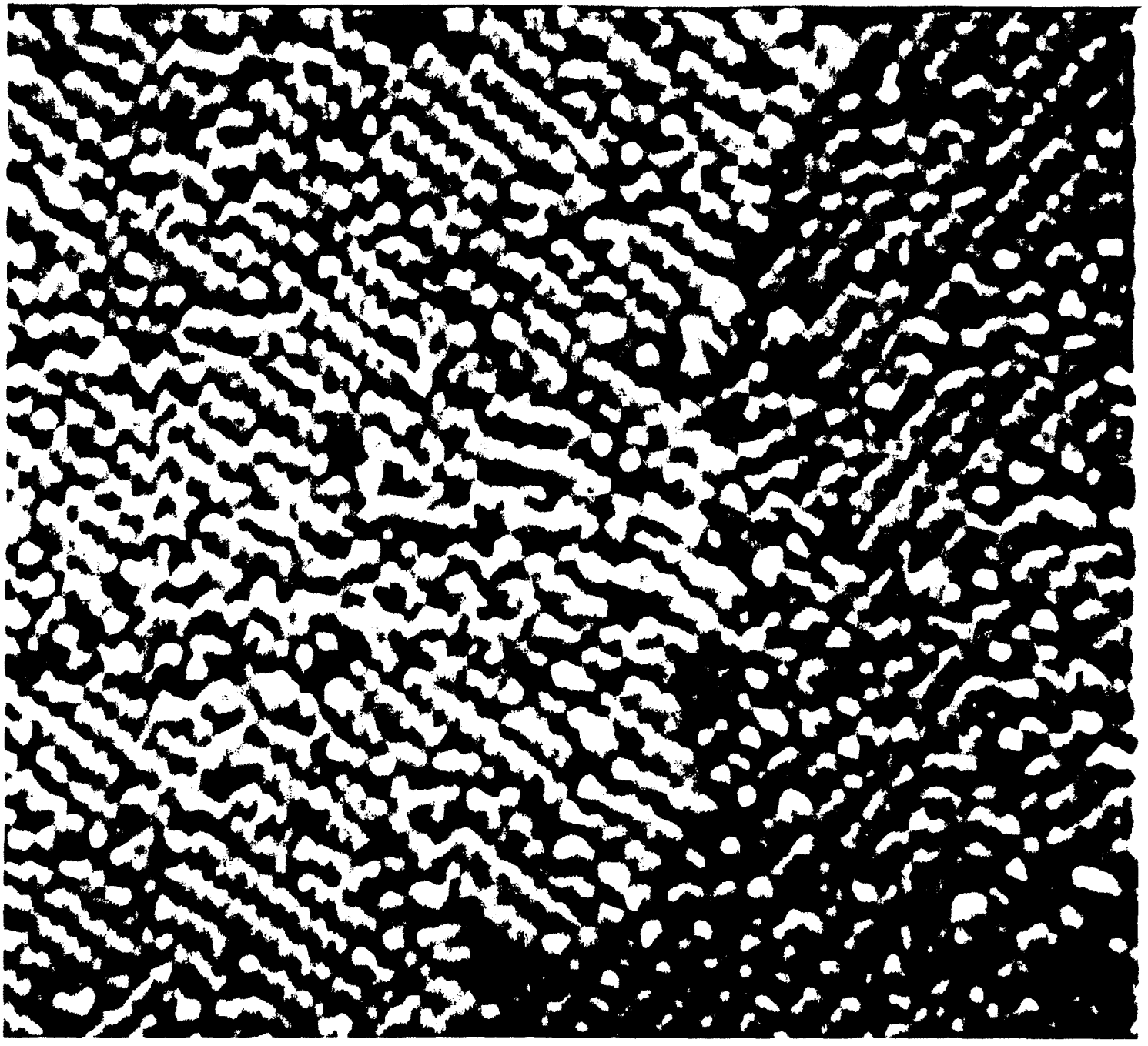

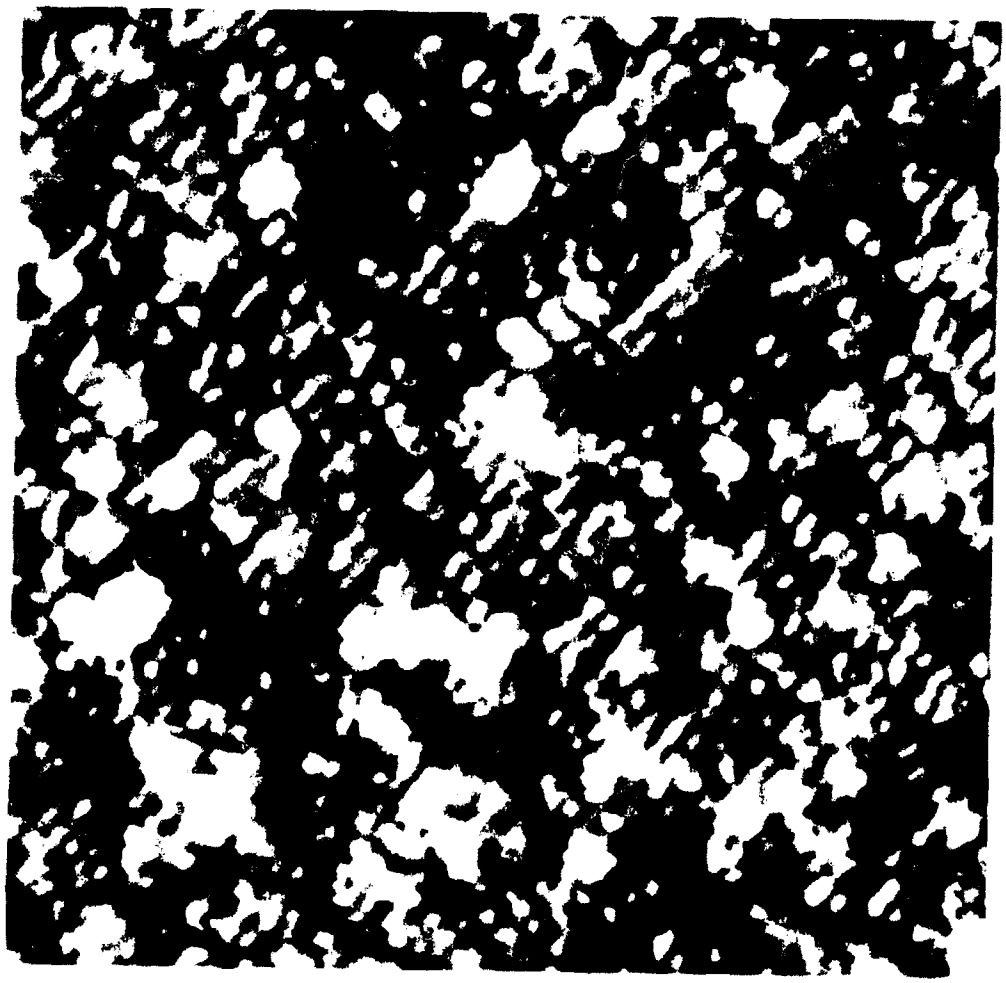

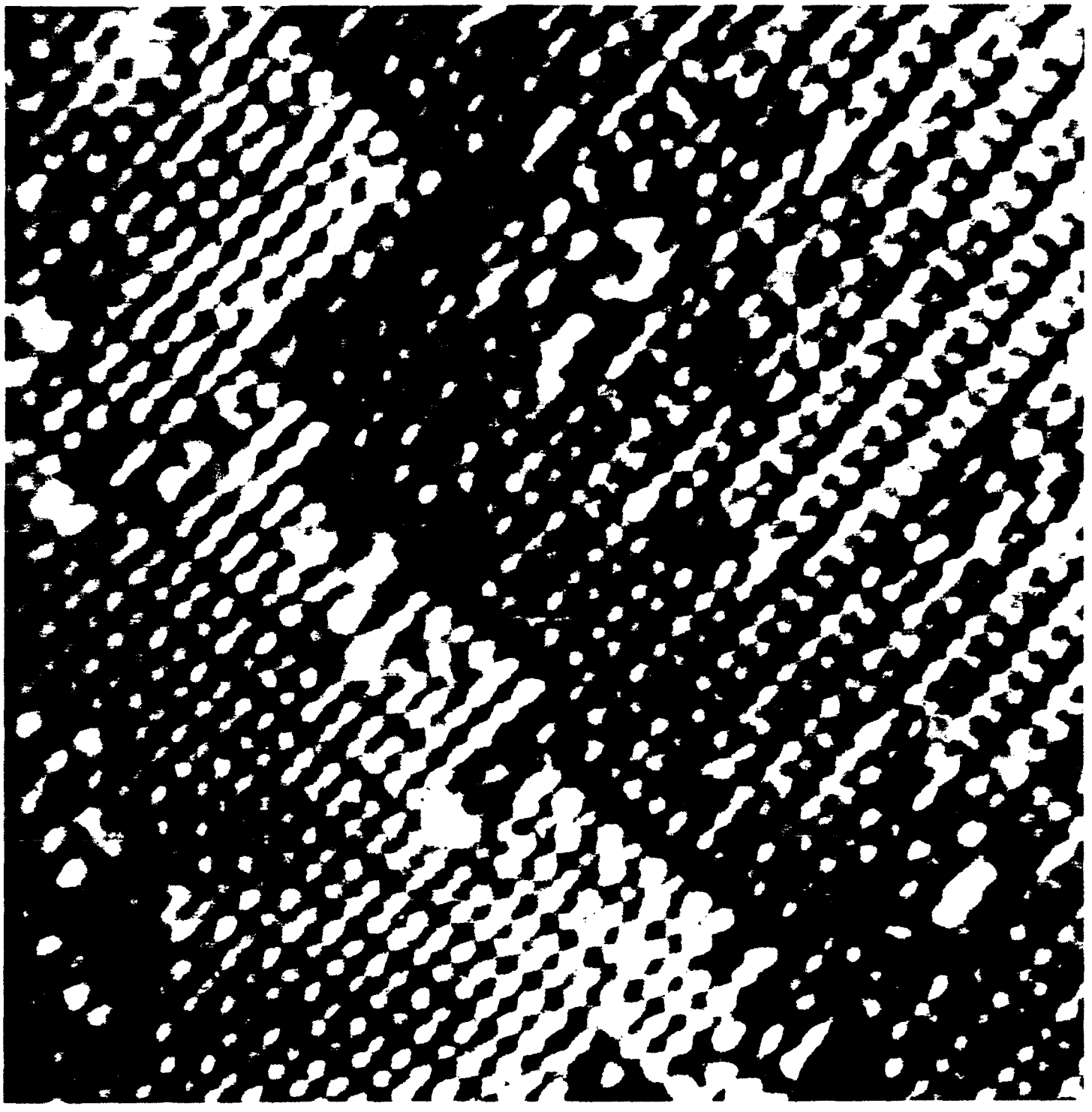

Fig. 4

Possible Bonding Sites on Si(001)(2X1) for Fragments of Si_2H_6

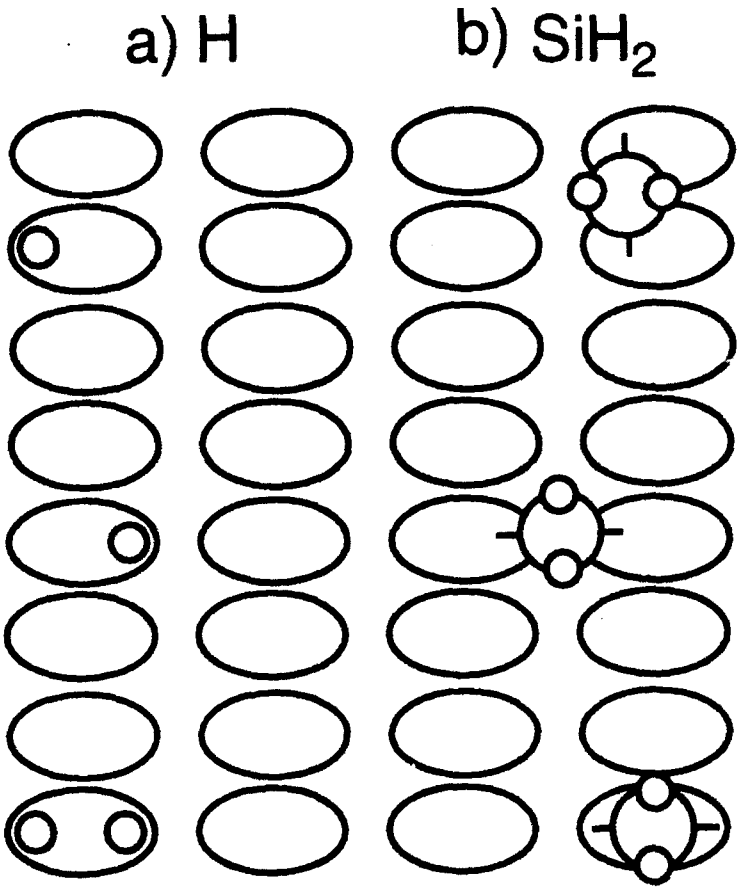

O = H_{ads}

= $SiH_{2,ads}$

= Si-Si dimer

Fig. 5

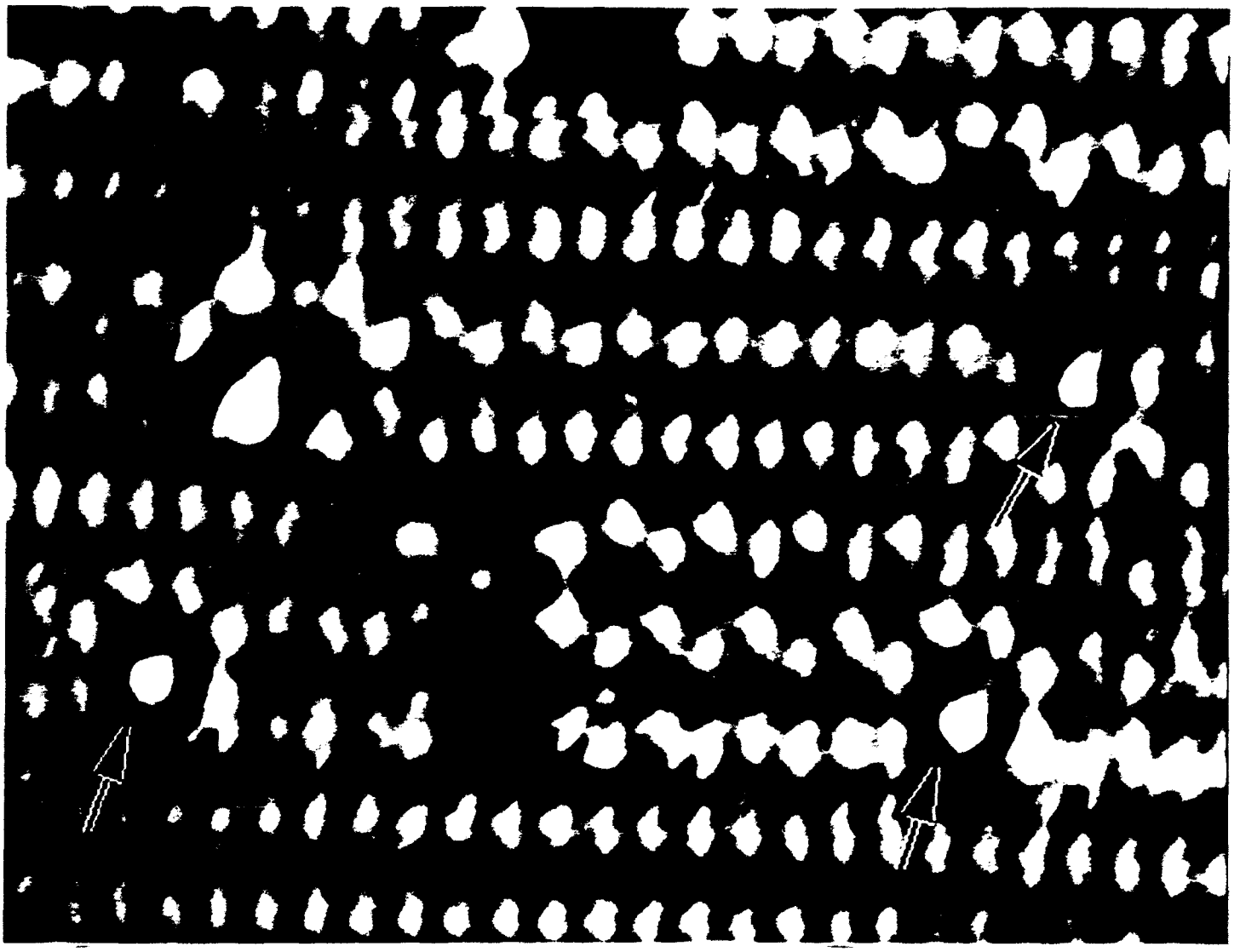

Fig. 6

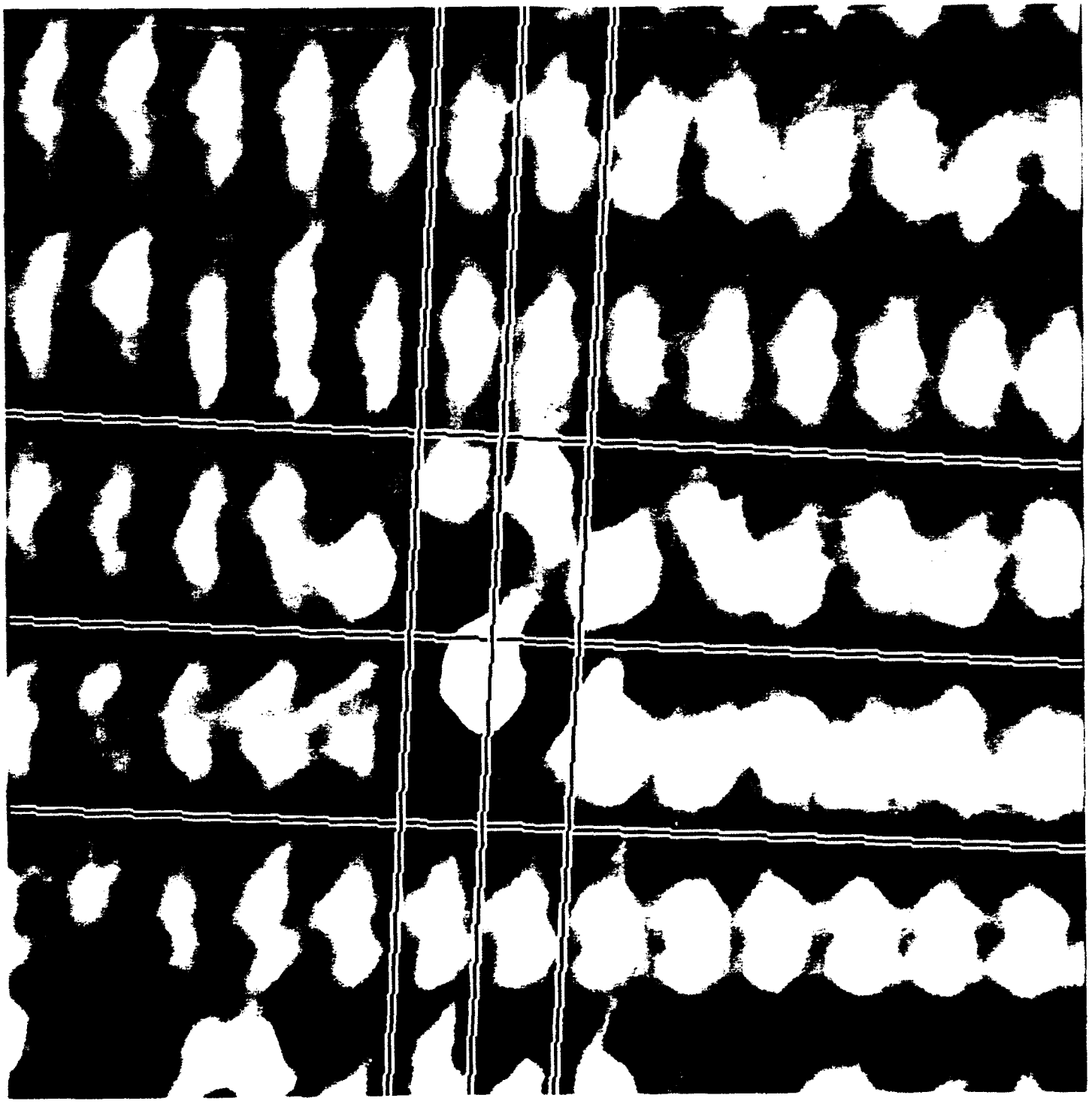

Fig 7

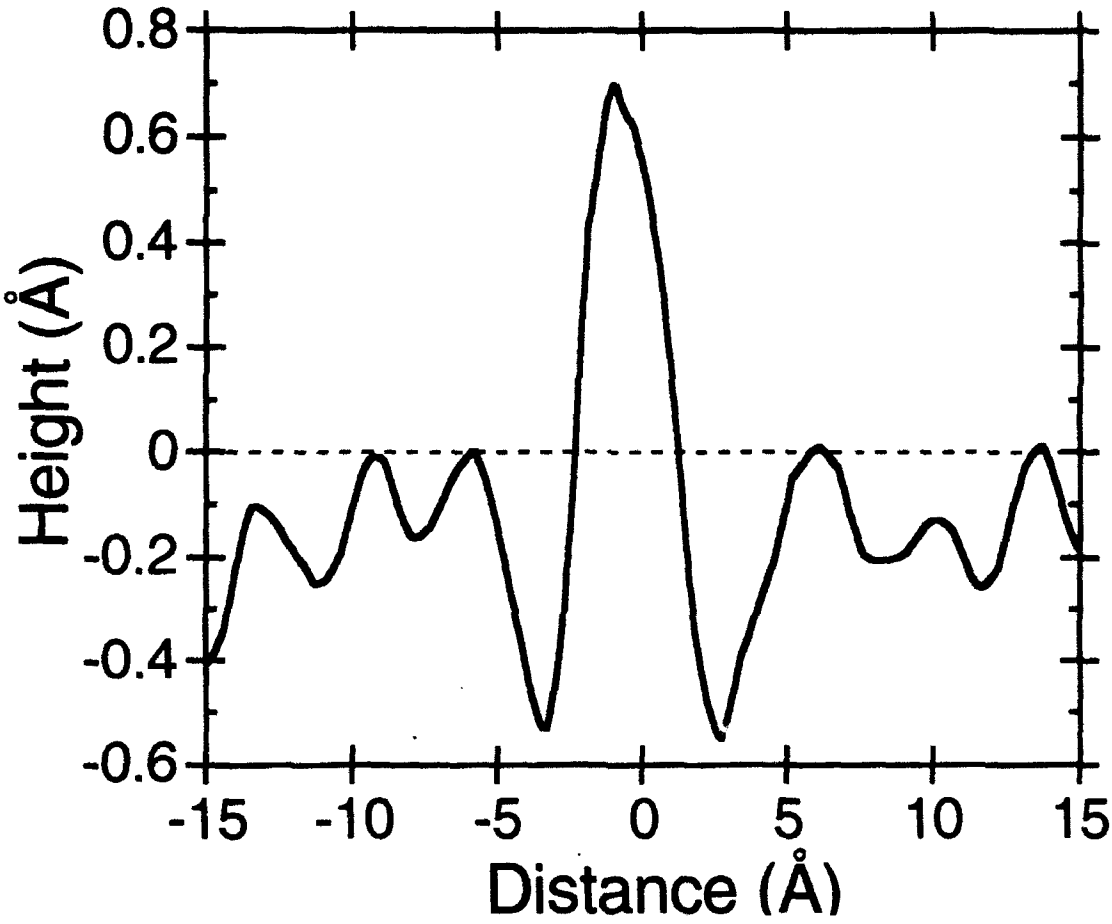

Fig. 8

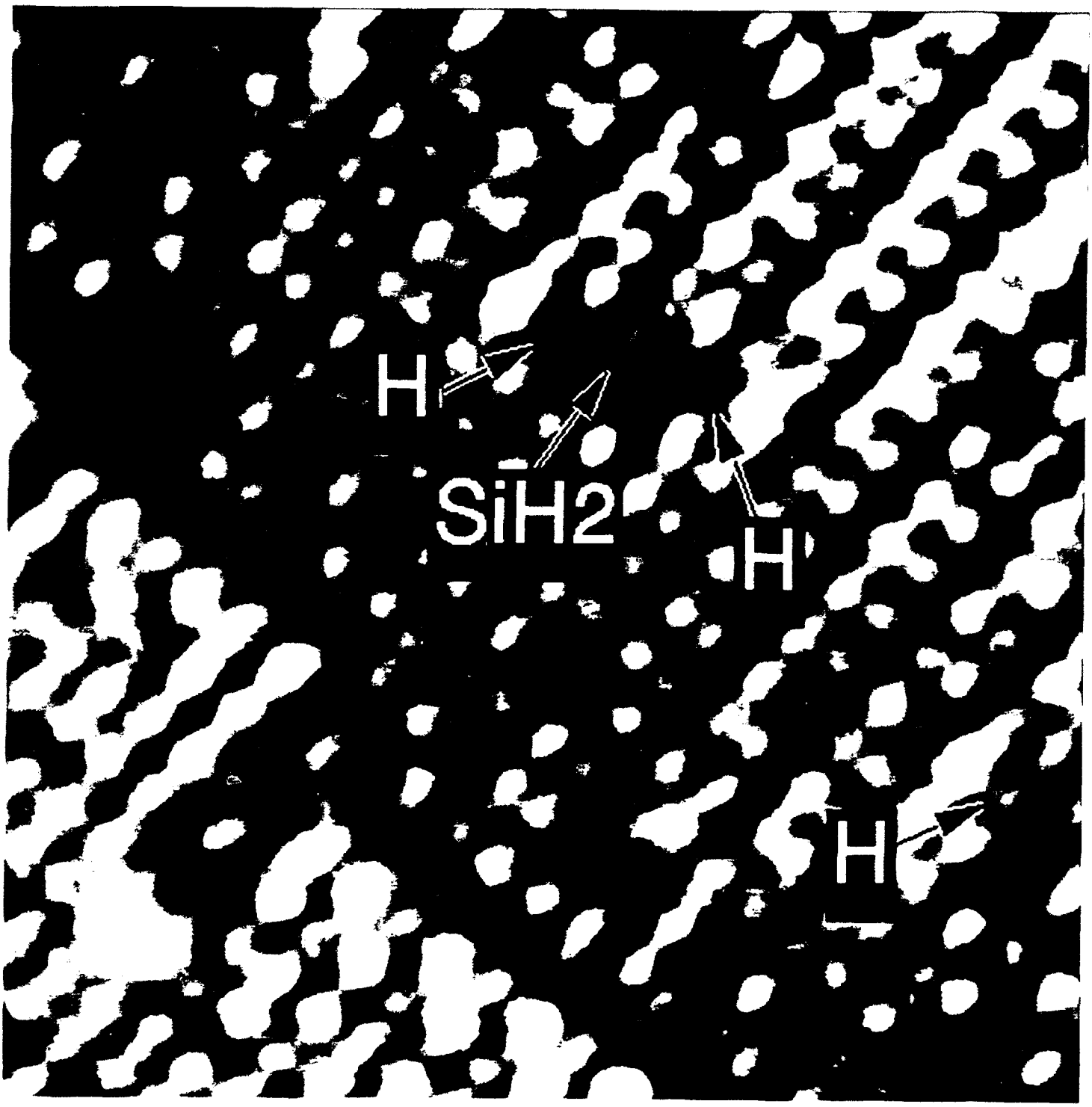

Fig. 9

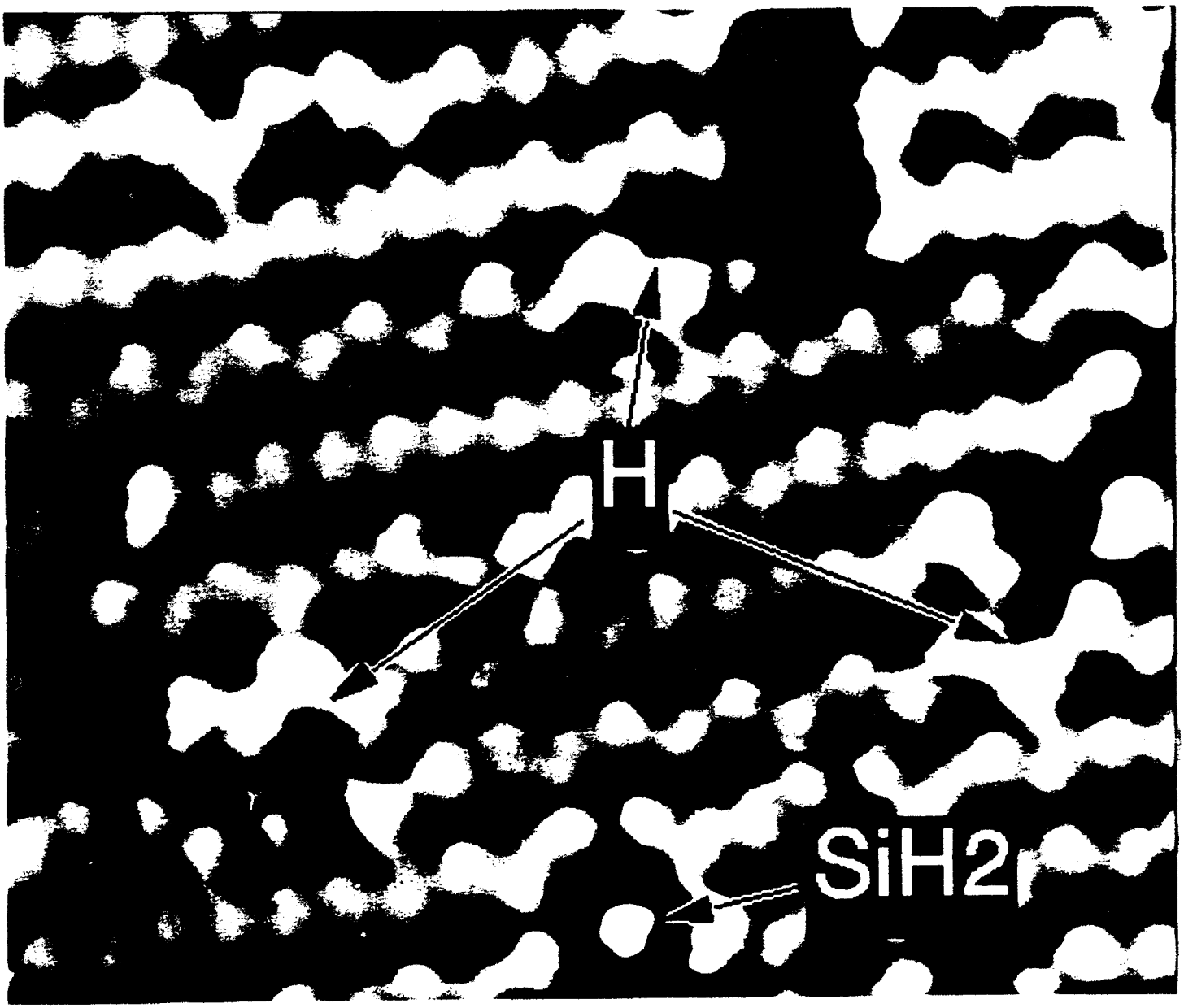

Fig. 10

Fig. 11

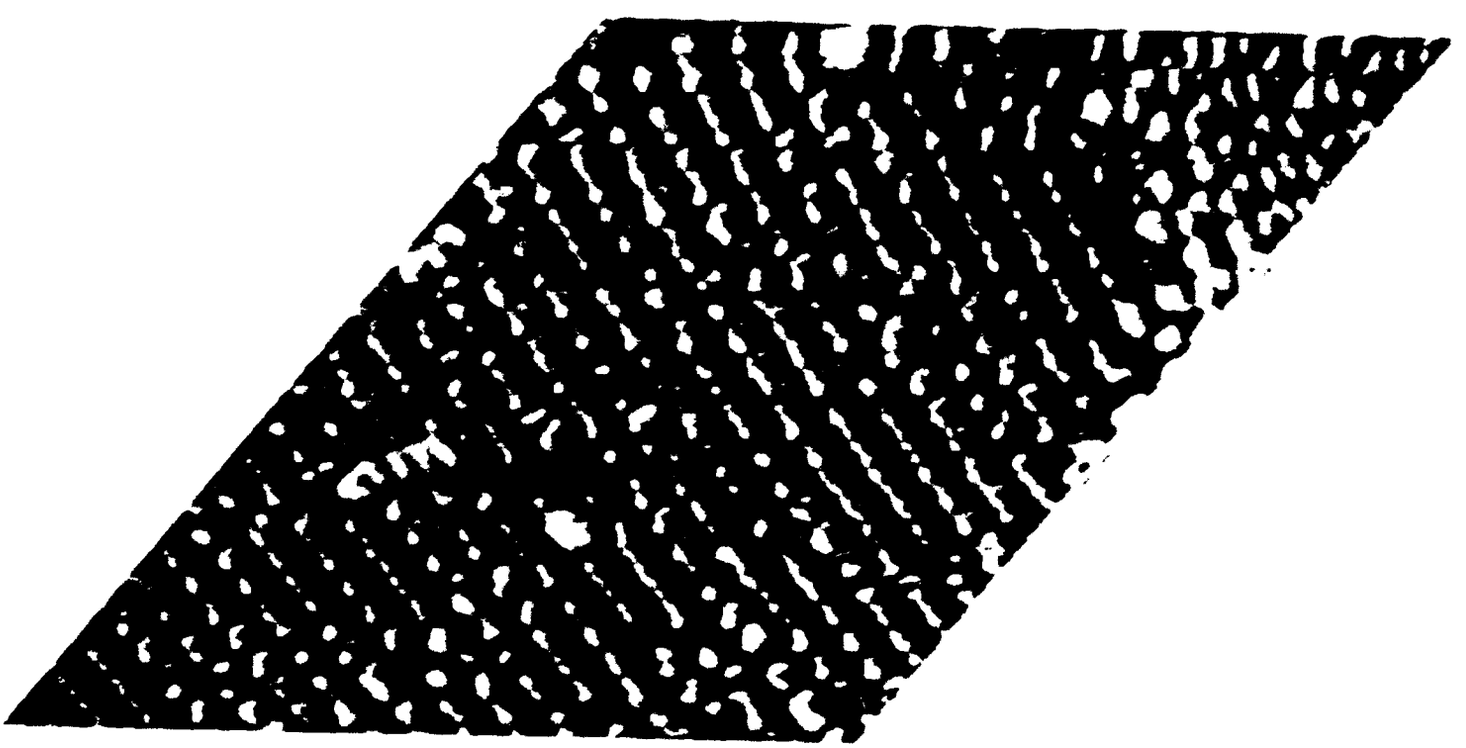

Fig. 12

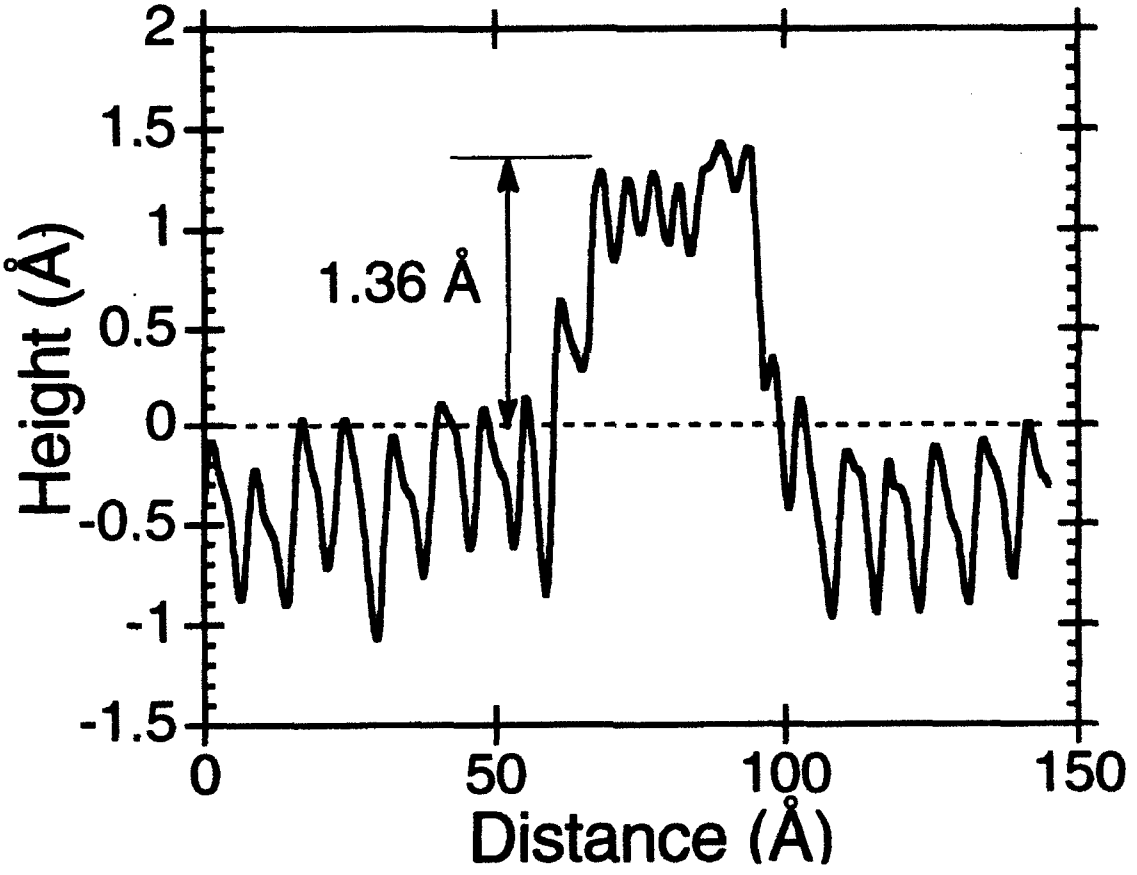

Fig. 13

Fig. 14